Mechanisms for optical nonlinearities and ultrafast carrier dynamics in Cu_xS nanocrystals

Victor I. Klimov*
Chemical Sciences and Technology Division, Los Alamos National Laboratory, Los Alamos, New Mexico 87545

Vladimir A. Karavanskii
Institute of General Physics, 38 Vavilov Street, 117942 Moscow, Russia
(Received 11 April 1996; revised manuscript received 7 June 1996)

Mechanisms for optical nonlinearities and ultrafast carrier dynamics in Cu_xS nanocrystals (NC's) are studied using femtosecond pump-probe techniques and nanosecond *Z*-scan measurements. Depending on the copper deficiency, transient absorption is dominated either by state-filling-induced bleaching [for copper sulfide phases with $x = 1.8$ (digenite), 1.9, and 1.96 (djurleite)] or by photoinduced absorption [$x = 2$ (chalcosite)]. This difference is explained in terms of the change in the dominant nonlinear-optical mechanism resulting from an indirect-direct-gap transformation accompanying the increase in copper deficiency. Extremely fast signal relaxation (on the time scale from 400 fs to 4 ps) observed in the initial stage after excitation is attributed to carrier trapping. The existence of different types of nonlinearities in Cu_xS NC's formed by direct- and indirect-gap phases of copper sulfide is confirmed by results of the *Z*-scan measurements. [S0163-1829(96)06934-2]

I. INTRODUCTION

Three-dimensional (3D) carrier confinement in semiconductor nanocrystals (NC's) results in size-dependent photoluminescence (PL) and absorption spectra, and significantly modifies nonlinear optical properties[1,2] and carrier dynamics[3,4] with respect to those in bulk materials. So far, most experimental and theoretical studies have concentrated on NC's formed by direct-gap II-VI semiconductors such as CdS and CdSe (see, e.g., Refs. 3–6). The nonlinear optical response in these systems is dominated by state-filling-induced bleaching peaked at positions of the allowed optical transitions.[2,7] Under certain conditions, less pronounced effects such as a two-pair Coulomb interaction[8,9] or a trapped-carrier-induced dc-Stark effect[10] can be also manifested in the nonlinear transmission of semiconductor NC's. The transmission recovery after picosecond or femtosecond excitation is usually nonexponential, with shortest components on the subpicosecond or picosecond time scales[8,11,12] This fast relaxation is usually explained in terms of carrier trapping[3,11] or Auger recombination.[12]

In our recent paper, we reported the preparation, linear and picosecond nonlinear transmission of NC's of a new type, namely, NC's formed by different copper sulfide phases.[13] The effect of 3D spatial confinement is clearly manifested in room-temperature linear absorption of these samples as distinct peaks at the positions of the allowed optical transitions coupling quantized electron and hole states. Depending on the copper deficiency, the energy band gap in copper sulfide varies from ~ 1.2 eV for $x = 2$ (chalcosite) (Refs. 14 and 15) to ~ 1.5 eV for $x = 1.8$ (digenite),[16] accompanied by a transformation of an originally indirect-gap semiconductor to a direct-gap one. These interesting properties, as well as small electron mass[13] resulting in large confinement-induced energy shifts, provide a broad phase/size-controlled tuning range and give an opportunity to compare the effects of 3D confinement on nonlinear optical properties in direct- and indirect-gap semiconductors.

In the present paper, we report on femtosecond transient absorption and *Z*-scan results in Cu_xS NC's. Both measurements indicate a drastic difference in the nonlinear optical response in NC's formed by direct- and indirect-gap phases of copper sulfide. The optical nonlinearities and ultrafast carrier dynamics in Cu_xS NC's are compared with those in CdS NC's.

II. SAMPLES AND EXPERIMENTAL PROCEDURES

Copper sulfide NC's of ~ 4 nm radius are prepared by a CdS-to-Cu_xS chemical conversion from glasses originally containing CdS NC's (for preparation procedure see Refs. 13 and 17). The converted layers of 40–70 μm thickness are formed on one side of the source CdS-doped glasses. The unconverted part of the glass on the opposite side of the samples is removed by polishing. In the present paper we report on three types of samples. Two of them are almost monophase and contain NC's of copper sulfide in the copper nondeficient phase with $x = 2$ (chalcosite, sample 1) and the phase with $x = 1.8$ corresponding to the maximum copper deficiency (digenite, sample 2). Sample 3 is a mixture of NC's in different copper sulfide phases with $x = 2$, 1.96, 1.9, and 1.8. Uncontrolled oxidation during the preparation does not allow at present the fabrication of monophase samples with intermediate copper deficiencies $x = 1.9$ and 1.96 (djurleite).

Femtosecond nonlinear transmission of the samples is studied by two different pump-probe experiments. In the first, the sample is probed with broad-band pulses of a femtosecond continuum that provides information on the spectral distribution of the nonlinear optical response over a broad spectral range (0.4–1 μm). The other method is based on a single-wavelength fast-scan technique,[18] which allows precise measurements (accuracy up to 10^{-7}) of the buildup and relaxation dynamics of the transient absorption with femtosecond time resolution.

In the measurements with a femtosecond continuum, the

samples are excited at 3.1 eV by frequency-doubled pulses from a regeneratively amplified mode-locked Ti-sapphire laser (Clark-MXR NJA-4 oscillator coupled to the CPA-1000 amplification system). The pulse duration is 100 fs, the maximum pulse energy is 1 mJ, and the repetition rate is 1 kHz. Pump-induced transmission changes are probed by delayed pulses of a femtosecond continuum generated in a 1-mm-thick sapphire plate. A 0.15-m spectrometer and a liquid-nitrogen-cooled charge-coupled device are used to measure the transmission in the absence (T_0) and in the presence (T) of the pump, from which we derive the differential transmission spectra (DTS): $D=(T-T_0)/T_0=\Delta T/T_0$. In the small signal limit ($D \ll 1$) the differential transmission is proportional to the absorption change $\Delta\alpha$: $D \approx -\Delta\alpha d$ (d is the sample thickness).

In fast-scan measurements, 80-fs pulses from a Ti-sapphire oscillator (Spectra-Physics Tsunami) are split into pump and probe beams which are focused onto the sample. To minimize the effect of the coherent artefact[19] the probe and the pump beams are cross-linear polarized. The probe pulses are rapidly scanned with respect to the pump pulses using a shaker driven at the frequencies of 40–90 Hz. The incident and the transmitted probe pulses are detected with large area silicon p-i-n photodiodes and differentially amplified to reduce the effect of fluctuations in the laser intensity and allow background-free detection of the nonlinear signal. The amplified signal is coupled to a fast digital acquisition board which can sample and average over 10^5 scans in approximately 10 min.

Open aperture Z-scan measurements[20] are done using a pulsed dye laser (Quanta Ray PDL-3) pumped by a frequency doubled Nd:YAG laser (Quanta Ray GCR-3). The pulse duration is around 6 ns and the repetition rate is 10 Hz. The pump beam is split into signal and reference channels, and the signal beam is focused with a 150-mm lens onto the sample with a spot diameter 16 μm. The signal pulses (after transmission through the sample) and the reference pulses are detected with large area silicon p-i-n photodiods coupled to a boxcar averager. To reduce the effect of sample nonuniformity in the plane, perpendicular to a Z-direction, each scan is normalized to a baseline taken at low laser intensity in the regime of linear transmission. To derive the absolute values of nonlinearity the data are calibrated using a reference ZnSe sample.

All measurements reported below are performed at room temperature.

III. LINEAR ABSORPTION SPECTRA

Figure 1 shows absorption spectra of converted glasses (samples 1, 2, and 3) in comparison to the absorption spectrum of the CdS-doped source glass. All three of the converted samples show an increase in the absorption coefficient and a redshift of the absorption edge with respect to that in CdS NC's. The absorption in Cu_2S NC's [sample 1; Fig. 1(a)] increases gradually with photon energy starting at $\sim$ 1.6 eV ($\sim$400-meV confinement-induced increase in the indirect energy gap with respect to that in bulk chalcosite)[14,15] and shows a step around 2.6 eV which can be explained by a contribution from transitions across the direct energy gap ($\sim$ 2.2 eV in bulk chalcosite).[21,22] Sample 2 shows two well-resolved peaks at 2.16 (ω_3) and 2.59 eV (ω_4) which can be assigned to transitions coupling the lowest electron and hole quantum-confined states of s (ω_3) and p (ω_4) symmetry in digenite NC's.[13] In addition to these two peaks, sample 3 (mixture of different phases) exhibits a bump around 2.69 eV (ω_5) and a broad maximum at 1.6–1.8 eV which can be decomposed into two Gaussian bands centered at 1.62 (ω_1) and 1.83 eV (ω_2). These additional features are attributed to NC's in the phases with $x = 1.9$ (ω_2) and $x = 1.96$ (ω_1, ω_5).[13]

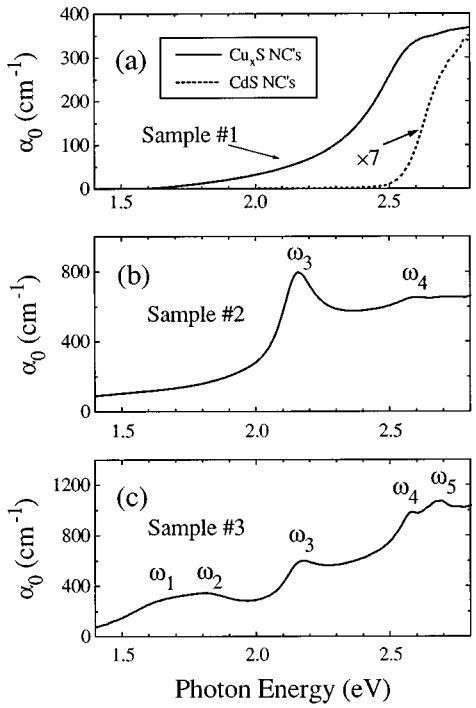

FIG. 1. Linear absorption spectra of Cu_xS NC's (solid lines) and the source CdS-doped glass (dashed line). The spectra taken for samples 1 (phase with x =2), 2 (x = 1.8), and 3 (mixture of phases) are denoted as (a), (b), and (c), respectively.

The contributions from phases with $x = 2$ and $x = 1.96$ are difficult to separate in linear absorption because of the small ($\sim$30 meV) difference in the band-gap energies. In our previous paper (Ref. 13), we tentatively assigned the bands ω_1 and ω_5 to the phase with $x = 2$ based on the spectral structure of the absorption in the mixed samples. However, the spectra of the monophase Cu_2S samples (not available at the time of experiments reported in Ref. 13) do not exhibit maxima around 1.6 and 2.7 eV. This shows that the bands ω_1 and ω_5 should be assigned to a phase with $x = 1.96$ (djurleite).

Summarizing the linear absorption data, we can conclude that NC's in the phase with $x = 2$ (indirect-gap semiconductor in the bulk form) do not show well pronounced discrete features in absorption spectra, whereas the NC's formed from direct band-gap phases ($x = 1.96$, 1.9, and 1.8) exhibit several well-resolved peaks. In particular, the peaks at ω_1, ω_2, and ω_3 mark the positions of the lowest optical transitions between spatially confined electron and hole states (NC energy band gap) in NC's composed of copper sulfide phases with x=1.96, 1.9, and 1.8, respectively.

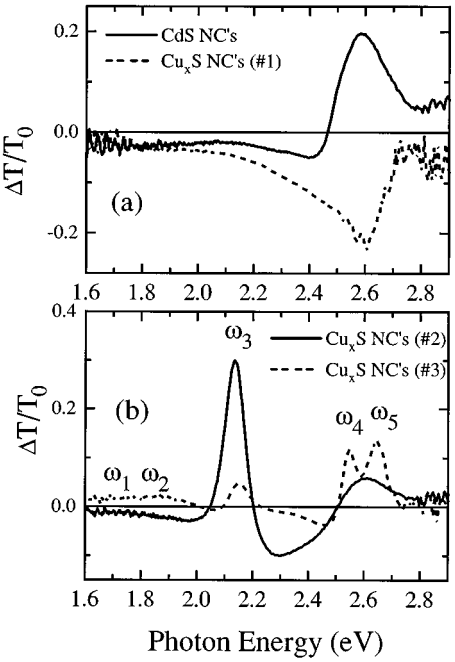

FIG. 2. DTS taken at $\Delta t = 2$ ps for converted samples 1 (a), 2 and 3 (b) in comparison to the DTS in the source CdS-doped glass (a). Pump fluence $j_p = 9$ mJ cm^{-2}.

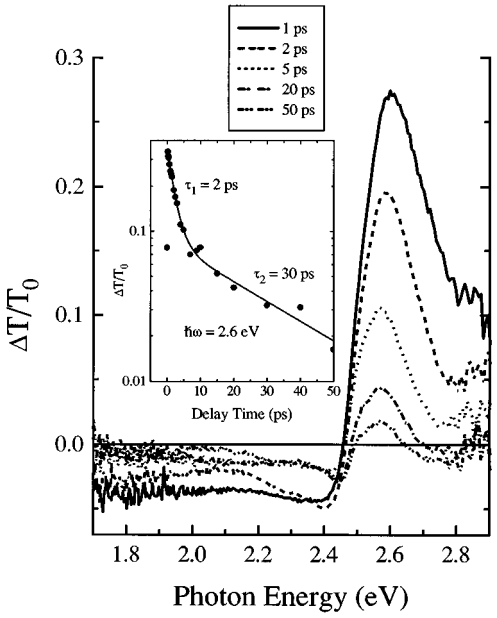

FIG. 3. DTS taken for CdS NC's at different delay times after excitation ($j_p = 9$ mJ cm^{-2}). Inset shows time dependence of photoinduced absorption changes at 2.6 eV.

IV. DIFFERENTIAL TRANSMISSION SPECTRA

Figure 2 shows the DTS measured for three different samples of Cu$_x$S NC's at 1 ps after excitation (pump fluence $j_p = 9$ mJ cm^{-2}). For comparison the spectrum of the CdS-doped source glass is shown also [Fig. 1(a); solid line]. The differential transmission in CdS NC's is dominated by bleaching located at the position of the lowest $s_e - s_h$ transition. In contrast, the DTS of copper sulfide NC's with $x = 2$ only show a broad band of photoinduced absorption peaked around 2.6 eV. The Cu$_x$S NC's in copper-deficient phases [samples 2 and 3; Fig. 2(b)] exhibit a number of bleaching bands, located at the positions of the discrete features seen in linear absorption. These bands are superimposed on a broad negative background, indicating the significant role of excited-state absorption. Similar structureless photoinduced absorption is also observed in CdS NC's at spectral energies $\hbar\omega < 2.5$ eV [see Fig. 2(a)], and was previously reported for CdSe NC's (see, e.g., Refs. 7 and 23). In copper sulfide NC's with $x = 1.8$ (sample 2), the bleaching bands at ω_3 and ω_4 mark two lowest intense $s_e - s_h$ and $p_e - p_h$ transitions. The mixed sample 3 exhibits additional weak broad bleaching at $\omega_1 - \omega_2$ spectral energies (the lowest optical transitions in NC's with $x = 1.96$ and 1.9, respectively) and a sharp feature at ω_5 (transition involving a higher-lying excited state in djurleite NC's).

The next three figures show the DTS dynamics in the source CdS-doped glass (Fig. 3) and in the modified monophase glasses [Figs. 4 (sample 2) and 5 (sample 1)]. The DTS in CdS NC's at short delay times ($\Delta t < 50$ ps) are dominated by bleaching of the lowest transition between electron and hole quantized states. Due to a large difference between electron and hole masses in CdS ($m_h/m_e \sim 6$), quantized levels in a valence band are much more closely spaced than those in a conduction band. Therefore, room-temperature occupation numbers for the lowest hole states are significantly smaller than those for the lowest $1S_e$ electron state.[24] The latter means that the state-filling-induced bleaching of the lowest transition and its dynamics are dominated by an electron contribution. This is confirmed by measurements of transmission recovery in CdSe NC's, which show the same dynamics for bleaching bands originating from occupied A- and unoccupied C-valence subbands.[7,24] Thus, the bleaching decay (at least in its initial stage) mea-

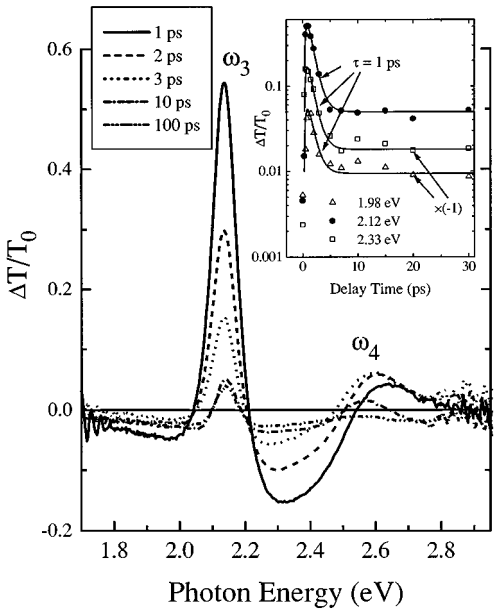

FIG. 4. DTS taken for Cu$_x$S NC's (sample 2) at different delay times after excitation ($j_p = 9$ mJ cm^{-2}). Inset shows time dependence of photoinduced absorption changes at 1.98, 2.12, and 2.33 eV.

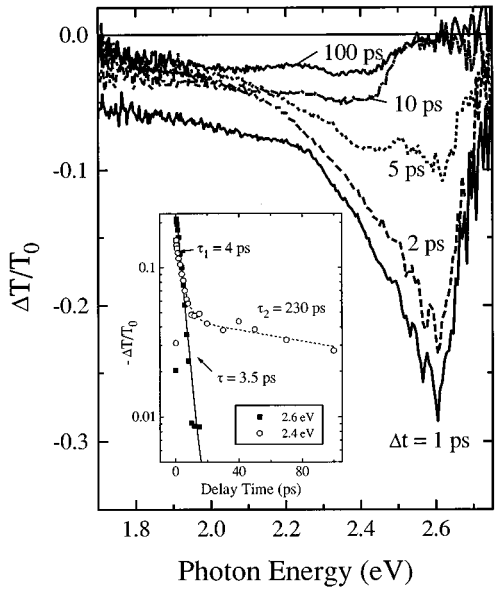

FIG. 5. DTS taken for Cu_xS NC's (sample 1) at different delay times after excitation (j_p = 9 mJ cm^{-2}). Inset shows time dependence of photoinduced absorption changes at 2.4 and 2.6 eV.

sured in the present experiments reflects the change in the occupation of the lowest electron quantized level. At low pump fluence ($j_p <$ 1 mJ cm^{-2}), short-term relaxation dynamics of bleaching observed in CdS NC's are almost monoexponential, with a time constant in the range from 15 to 25 ps. This decay can be assigned to an electron trapping, in agreement with results of the time-resolved PL measurements,[3] indicating the electron trapping on the time scale of tens of ps. With increasing pump intensity above 1 mJ cm^{-2} the initial decay gets faster and transmission recovery dynamics become nonexponential (see inset to Fig. 3). Double exponential fits to experimental transients taken at different pump intensities show that the fast relaxation constant is pump-fluence dependent and shortens to 1.5 ps at 12 mJ cm^{-2} . This fast pump-intensity-dependent decay is usually explained in terms of nonradiative Auger recombination (see, e.g., Refs. 25 and 26). An alternative explanation of this decay as due to stimulated emission can be definitely ruled out because the maximum absorption change ($|\Delta\alpha|/\alpha_0$) did not exceed 0.5, being thus below the gain threshold ($|\Delta\alpha|/\alpha_0 = 1$).

At $\Delta t >$ 50 ps, the differential transmission in CdS NC's instead of well-pronounced bleaching shows a weak feature which resembles the first derivative of a Gaussian (Lorentzian) peak. This is a signature of a low-energy shift of the optical transition, which can result from a buildup of a dc-electric field following a spatial separation of negative and positive charges due to their localization. This effect is usually referred to as a trapped-carrier-induced dc-Stark effect and was previously reported for II-VI NC's.[10]

Time-resolved DTS for digenite NC's are shown in Fig. 4. As in CdS NC's, the DTS are dominated by bleaching of the lowest transition (band ω_3) at short times after excitation ($\Delta t <$ 5 ps) and show approximately the same amplitudes of bleaching and increased absorption at longer delays between pump and probe pulses, which is indicative of the change in the mechanism for nonlinearity from the state-filling to the dc-Stark effect.

The inset to Fig. 4 shows the dynamics of differential transmission derived from measured DTS for main bleaching band ω_3 (solid circles) and two regions of increased absorption above (open squares) and below (open triangles) of the ω_3 transition. The bleaching relaxation can be fit to a monoexponential decay (τ = 1 ps) with a very slow background. The DTS shape in the region of the ω_3 and ω_4 transitions at $\Delta t >$ 5 ps is typical for the shift of optical transitions, suggesting that at the end of the fast relaxation both carriers (an electron and a hole) are trapped into localized states. The fast monoexponential bleaching relaxation is indicative of extremely effective electron trapping with a rate significantly exceeding that in CdS NC's.

Both increased absorption features at 2.33 and 1.98 have the same buildup and relaxation dynamics (see inset to Fig. 4), indicating that increased absorption most likely forms a single band (in the range from ~1.8 to ~2.5 eV) which represents a background for relatively narrow bleaching bands at ω_3 and ω_4. Interestingly, this broad-band absorption evolves in the same way as bleaching of the ω_3 transition (see inset to Fig. 4), which shows that both effects are dominated by the same species, namely, by the electrons in the lowest quantized state. These electrons contribute to bleaching by a state-filling effect, whereas their contribution to excited state absorption is most likely due to intraband transitions (see discussion below).

As mentioned above, increased absorption is the only effect seen in chalcosite NC's. Chalcosite is an indirect-gap material in the bulk form. In low-dimensional semiconductors, due to confinement-induced mixing of states, optical transitions across originally an indirect energy gap can be allowed in the first order of the perturbation theory. However, calculations performed, e.g., for Si NC's,[27,28] show that the probability of these transitions remains low unless the NC size is smaller than 2–3 nm. Therefore, one can hardly expect a large confinement-induced increase in absorption in case of the relatively large Cu_2S NC's (~ 8 nm in diameter) studied in the present experiments. This can explain the absence of sharp features in linear absorption and pronounced bleaching bands in DTS in NC's of this type.

The nonlinear optical response in indirect-gap semiconductors such as Si is dominated by free-carrier absorption.[29] The analogous effect—intraband transitions between quantized levels, can be significantly enhanced in quasi-zero-dimensional structures,[30] leading to large excited-state absorption. According to calculations in Ref. 30, even in relatively large NC's with sizes in the range of tens of nm, spatial confinement has a significant effect on intraband transition probabilities. The excited-state absorption due to intraband transitions most likely dominates the nonlinear optical response in Cu_2S NC's.

The time-resolved DTS for these NC's are shown in Fig. 5. The DTS dynamics (see inset to Fig. 5) reveal the presence of two components. One of them (peaked at 2.6 eV and having a long low-energy tail) is very fast, with a relaxation constant of ~4 ps. The other component (broad feature in the region below 2.5 eV) is much slower and has a decay constant about 230 ps. The short relaxation constant is typical for carrier trapping. Therefore, short-lived DTS compo-

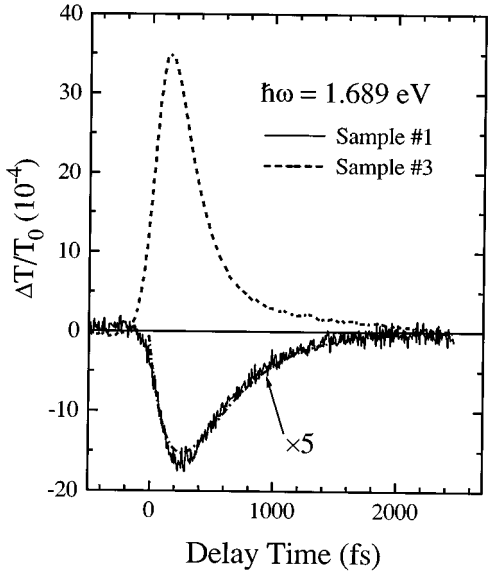

FIG. 6. Time transients taken for samples 1 (solid line) and 2 (dashed line) at 1.689 eV ($j_p = 80\ \mu J\ cm^{-2}$). The dashed-dotted line shows a fit to the experimental data measured for sample 1.

nent can be attributed to carriers occupying the lowest extended NC states, whereas the long-lived feature can be explained by excited-state absorption associated with localized carriers.

In addition to new features demonstrated in nonlinear transmission (particularly in the case of the phase with $x = 2$) the copper sulfide NC's allow a low-energy extension of the spectral range covered by II-VI NC's. In particular, the phase with $x = 1.96$ has the lowest transition in the near-IR region that facilitates the study of resonant optical nonlinearities using fundamental radiation from well-developed femtosecond Ti-sapphire lasers. An example of this kind of study is demonstrated in the next section.

V. FEMTOSECOND FAST-SCAN MEASUREMENTS

The fast-scan measurements are performed for several spectral energies from the region 1.55–1.69 eV, which corresponds to the absorption tail in Cu_2S NC's and falls into the pronounced absorption band ω_1 attributed to the phase with $x = 1.96$ (djurleite). Sample 2 ($x = 1.8$) does not show any detectable signal in the above spectral range. At $\hbar\omega = 1.689$ eV (Fig. 6), the differential transmission is negative (photoinduced absorption) in the chalcosite NC's (sample 1) and positive (photoinduced bleaching) in the mixed sample (sample 3). Variation in the laser photon energy does not affect significantly the temporal behavior of differential transmission in Cu_2S NC's but largely modifies the time transients in the case of the mixed sample (Fig. 7). In going to lower spectral energies, the signal gradually changes from bleaching to increased absorption. The spectral positions of the pump suggests that the main contributions to differential transmission in the mixed sample arise from djurleite and chalcosite NC's. The djurleite-related component is expected to be positive in the vicinity of the ω_1 resonance whereas the contribution from chalcosite NC's is negative in the whole spectral range (see previous section). The competition between these two components explains well the measured transients. For higher spectral energies the nonlinear signal is dominated by state-filling-induced bleaching in NC's with $x = 1.96$ (with possible contribution from the ω_2 bleaching in the phase with $x = 1.9$). A decreasing photon energy leads to an increasing contribution from chalcosite-related photoinduced absorption.

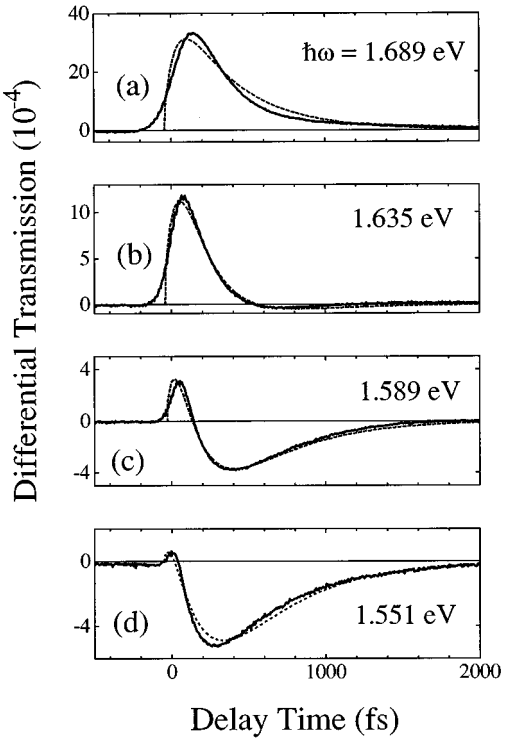

FIG. 7. Time transients taken for sample 3 ($j_p = 80\ \mu J\ cm^{-2}$) at spectral energies 1.689 (a), 1.635 (b), 1.589 (c), and 1.551 eV (d) (solid lines). Dashed lines show fits to the experimental data (see text).

We have modeled the measured time transients assuming the presence of two components (with positive and negative signs) with exponential buildup and decay dynamics: $y = \Sigma_{i=1}^{2} a_i (1 - e^{-t/\tau_{ri}}) e^{-t/\tau_i}$, where τ_{ri} and τ_i are the rise and decay times, respectively. To fit the data for the mixed sample we apply a two-stage fitting procedure. First, we derive the rise (τ_{r1}) and decay (τ_1) times characteristic of chalcosite NC's by fitting the time transients measured for monophase chalcosite samples to a single component function with exponential buildup and decay dynamics (see Fig. 6). As a result we get $\tau_{r1} = 450$ fs and $\tau_1 = 380$ fs. Then, we use the two component function with τ_{r1} and τ_1 fixed to fit the data taken for the mixed sample.

The results of the fitting procedure for sample 3 are shown in Fig. 7 by dashed lines. We were able to achieve reasonable agreement between the model and the measured data with τ_{r2} and τ_2 only slightly varying with spectral energies: $\tau_{r2} = 80$–100 fs and $\tau_2 = 390$–420 fs. The time τ_{r2} is close to our resolution and should be considered as an upper limit for the actual risetime of the bleaching component. The spectral distribution of the amplitudes for negative (a_1) and positive (a_2) components are shown in Fig. 8. The amplitude a_1 increases gradually with spectral energy, whereas a_2 is peaked at the position of the ω_1 absorption

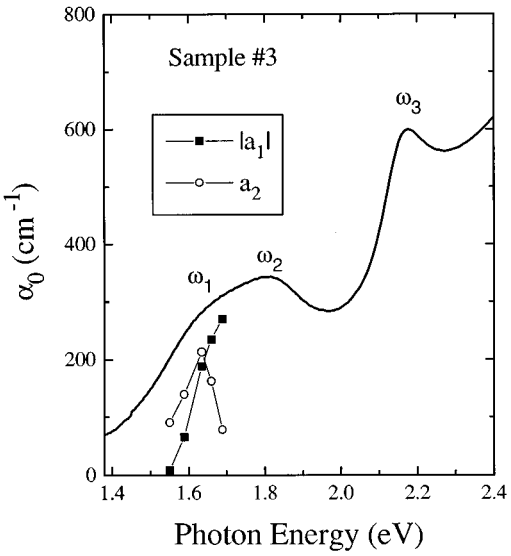

FIG. 8. Spectral distributions of amplitudes for negative (a_1) and positive (a_2) components of differential transmission in the mixed sample (derived from the fast-scan data) in comparison to the absorption spectrum in this sample.

indicating a dominant contribution from djurleite NC's to the photoinduced bleaching.

As expected for single-wavelength measurements, the state-filling-induced bleaching appears almost instantaneously with the pump (τ_{r2} = 80–100 fs), whereas the signal of increased absorption is noticeably delayed with respect to a laser pulse (τ_{r1} = 450 fs). This delay gives a measure of intraband relaxation into the states which are active in excited-state absorption in chalcosite NC's. Very fast relaxation constants ($\sim$400 fs) measured for both bleaching and increased absorption components are most likely determined by a combined action of two effects: intraband energy relaxation and ultrafast carrier trapping.

VI. NANOSECOND *Z*-SCAN MEASUREMENTS

Open aperture *Z*-scan measurements are performed at 1.82 eV on samples 1 and 3. *Z*-scan data taken for sample 1 (Fig. 9, open circles) only show the presence of one effect—photoinduced absorption, being characteristic of chalcosite NC's. The amplitude of the transmission dip increases almost linearly with laser pulse energy up to w_p = 18–20 μJ, and shows saturation at higher laser intensities.

The *Z* scans measured for the mixed sample (Fig. 9, solid squares) are dominated by photoinduced bleaching at low laser intensities, and clearly show the contribution from photoinduced absorption for pulse energies $w_p >$ 3–4 μJ (Fig. 10). These data (as the data of fast-scan measurements from the previous section) can be explained in terms of competition between two types of nonlinearities being characteristic of copper-sulfide phases with direct and indirect band gaps.

The laser photon energy is close to the ω_2 absorption maximum in copper sulfide NC's with x = 1.9. Therefore, state-filling-induced bleaching of the lowest optical transition in these NC's is likely to dominate the low-intensity nonlinear transmission in the mixed sample. With increasing

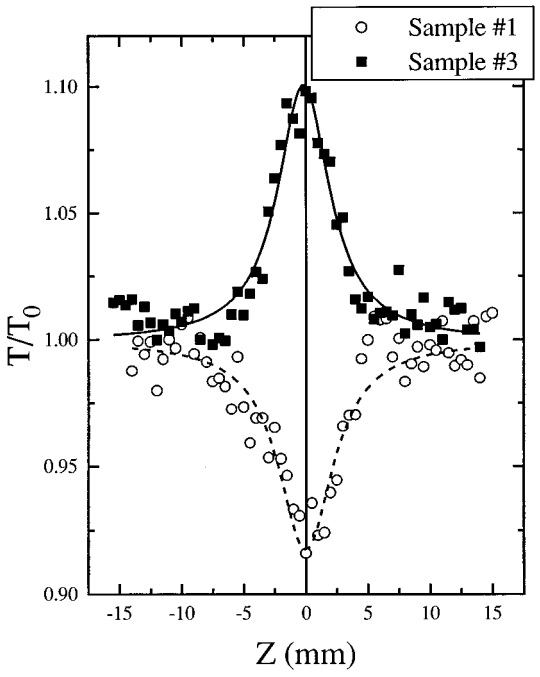

FIG. 9. Low-intensity open-aperture *Z*-scan data measured at 1.82 eV for samples 1 (open circles; w_p = 0.9 μJ) and 3 (solid squares; w_p = 9 μJ). Lines are fits to the experimental data (see text).

laser intensity up to $w_p \sim$ 3–4 μJ this transition gets saturated (analogous to the saturation effect in a resonantly excited two-level system). However, the above value is below the saturation threshold in chalcosite NC's ($w_p \sim$ 20 μJ) which are pumped not into the lowest excited state but into a higher one. Therefore, the photoinduced absorption in chal-

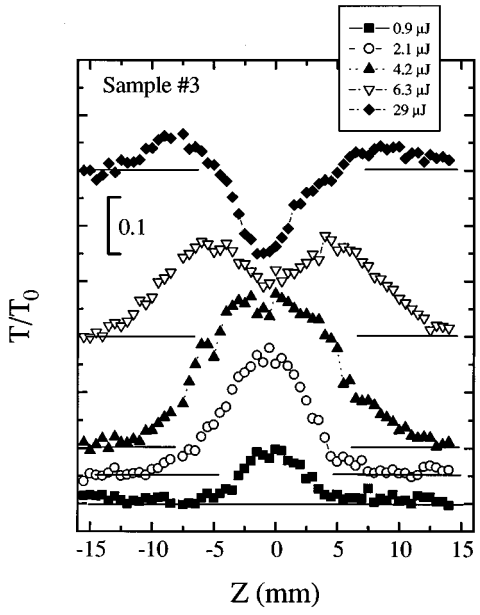

FIG. 10. Open-aperture *Z* scans measured for sample 3 at 1.82 eV for different laser pulse energies. To avoid intersections, the curves are arbitrarily shifted along the vertical axis (linear transmission levels for each of the *Z* scans are marked by horizontal lines).

cosite NC's tends to dominate the high-intensity response in the mixed sample.

To derive quantitative characteristics of the observed nonlinearities such as the Kerr type third-order nonlinear susceptibility ($\chi^{(3)}_{\text{eff}}$), we have fit the low-intensity Z-scan data assuming the following dependence of the absorption (α) on the laser intensity (I): $\alpha=\alpha_0+\beta I$, where α_0 and β are linear and nonlinear absorption coefficients, respectively (for details of the fitting procedure see, e.g., Ref. 20). The fit (Fig. 9, lines) yields the following values for the imaginary part of $\chi^{(3)}_{\text{eff}}$: 1.1×10^{-10} esu (sample 1) and -1.3×10^{-9} esu (sample 3). As expected, the mixed sample where the low-intensity response is determined by the direct-gap phase with $x = 1.9$ shows a much larger nonlinearity than the sample with NC's of the indirect-gap Cu_2S phase.

VII. CONCLUSIONS

We performed the extensive studies of optical nonlinearities and ultrafast carrier dynamics in Cu_xS NC's using femtosecond pump-probe techniques and nanosecond Z-scan measurements. Copper sulfide NC's with different copper deficiency are prepared by a CdS-to-Cu_xS chemical conversion from glasses originally containing CdS NC's. The measurements demonstrate a drastic difference in the nonlinear optical response in NC's formed by different copper sulfide phases. Depending on the copper deficiency, nonlinear transmission is dominated either by state-filling-induced bleaching ($x = 1.8$, 1.9, and 1.96) or by photoinduced absorption ($x = 2$). This is explained in terms of indirect-direct-gap transformation accompanying an increase in the copper deficiency which leads to a change in the dominant nonlinear-optical mechanism.

The temporal behavior of the transient absorption in phases with a direct band gap is similar to that in the source CdS-doped glass. It is dominated by state-filling-induced bleaching at short delay times between pump and probe pulses and shows an increasing contribution from a trapped-carrier-induced dc-Stark effect at longer delay times. The nonlinear optical response in NC's formed by the indirect gap phase ($x = 2$) only shows photoinduced absorption tentatively assigned to excited-state absorption due to intraband transitions.

The initial stage of transmission recovery is extremely fast in all types of copper sulfide NC's (subpicosecond or picosecond time scales) which is explained in terms of carrier trapping. Electron trapping dynamics in Cu_xS NC's are much faster than those in CdS NC's in the source glass.

Mixed samples containing NC's of different copper sulfide phases show very fast switching from bleaching to increased absorption (within less than 400 fs) which is explained in terms of competition between nonlinearities in NC's with direct and indirect energy gaps. This competition is also clearly manifested in Z-scan measurements as a change in the sign of the nonlinearity at high laser intensities.

ACKNOWLEDGMENTS

The authors thank D. McBranch and L. Smilowitz for technical assistance and critical reading of the manuscript. V. Karavanskii acknowledges the support from the Russian State Program ''Physics of Nanostructures'' (Grant No. I-042) and the Russian Basic Research Foundation (Grant No. 95-02-04510).

*Mailing address: CST-6, MS-J585, Los Alamos National Laboratory, Los Alamos, NM 87545. Electronic address: klimov@lanl.gov

[1] S. Schmitt-Rink, D. A. B. Miller, and D. S. Chemla, Phys. Rev. B **35**, 8113 (1987).
[2] B. Fluegel, M. Joffre, S. H. Park, R. Morgan, Y. Z. Hu, M. Lindberg, S. W. Koch, D. Hulin, A. Migus, A. Antonetti, and N. Peyghambarian, J. Cryst. Growth **101**, 643 (1990).
[3] V. Klimov, P. Haring-Bolivar, and H. Kurz, Phys. Rev. B **53**, 1463 (1996).
[4] J. Puls, V. Jungnickel, F. Henneberger, and A. Schülzgen, J. Cryst. Growth **138**, 1004 (1994).
[5] L. E. Brus, Appl. Phys. A **53**, 465 (1991).
[6] M. G. Bawendi, P. J. Carrol, W. L. Wilson, and L. E. Brus, J. Chem. Phys. **96**, 946 (1992).
[7] V. Klimov, S. Hunsche, and H. Kurz, Phys. Status Solidi B **188**, 259 (1995).
[8] V. Klimov, S. Hunsche, and H. Kurz, Phys. Rev. B **50**, 8110 (1994).
[9] K. I. Kang, A. D. Kepner, S. V. Gaponenko, S. W. Koch, Y. Z. Hu, and N. Peyghambarian, Phys. Rev. B **48**, 15 449 (1993).
[10] D. J. Norris, A. Sacra, C. B. Murray, and M. G. Bawendi, Phys. Rev. Lett. **72**, 2612 (1994).
[11] M. C. Nuss, W. Zinth, and W. Kaiser, Appl. Phys. Lett. **49**, 1717 (1986).
[12] J. Z. Zhang, R. H. O'Neil, and T. W. Roberti, Appl. Phys. Lett. **64**, 1989 (1994).
[13] V. Klimov, P. Haring Bolivar, H. Kurz, V. Karavanskii, V. Krasovskii, and Yu. Korkishko, Appl. Phys. Lett. **67**, 653 (1995).
[14] B. J. Mulder, Phys. Status Solidi A **15**, 409 (1973).
[15] P. S. McLeod, L. D. Partain, D. E. Sawyer, and T. M. Peterson, Appl. Phys. Lett. **45**, 472 (1984).
[16] B. J. Mulder, Phys. Status Solidi A **13**, 79 (1972).
[17] V. A. Fedorov, V. A. Ganshin, and Yu. N. Korkishko, Phys. Status Solidi A **139**, 9 (1993).
[18] W. A. Kütt, W. Albrecht, and H. Kurz, IEEE J. Quantum Electron. **28**, 2434 (1992).
[19] Z. Vardeny and J. Tauc, Opt. Commun. **39**, 396 (1981).
[20] M. Sheik-Bahae, A. A. Said, T.-H. Wei, D. J. Hagan, and E. W. Van Stryland, IEEE J. Quantum Electron. **26**, 760 (1990).
[21] E. Aperathitis, F. J. Bryant, and C. G. Scott, Sol. Energy Matter **20**, 15 (1990).
[22] S. B. Gadgil, R. Thangaraj, and O. P. Agnihotri, J. Phys. D **20**, 112 (1987).
[23] M. G. Bawendi, W. L. Wilson, L. Rothberg, P. J. Carroll, T. M. Jedju, M. L. Steigerwald, and L. E. Brus, Phys. Rev. Lett. **65**, 1623 (1990).
[24] S. Hunsche, T. Dekorsy, V. Klimov, and H. Kurz, Appl. Phys. B **62**, 3 (1996).
[25] M. Ghanassi, M. C. Schanne-Klein, F. Hache, A. I. Ekimov, D.

Ricard, and C. Flytzanis, Appl. Phys. Lett. **62**, 78 (1993).
[26] V. S. Dneprovskii, Al. L. Efros, A. I. Ekimov, V. I. Klimov, I. A. Kudriavtsev, and M. G. Novikov, Solid State Commun. **74**, 555 (1990).
[27] G. D. Sanders and Y.-C. Chang, Phys. Rev. B **45**, 9202 (1992).
[28] C. Delerue, G. Allan, and M. Lannoo, Phys. Rev. B **48**, 11 024 (1993).
[29] V. Grivikas, J. Linnros, A. Vigelis, J. Seckus, and J. A. Tellefsen, Solid State Electron. **35**, 299 (1992).
[30] V. Milanović and Z. Ikonić, Phys. Rev. B **39**, 7982 (1989).